X-ray Absorption Studies on the Mixed-Valence and Fully Reduced Forms of the Soluble Cu$_A$ Domains of Cytochrome *c* Oxidase

Ninian J. Blackburn,[*,†] **Simon de Vries,**[‡] **Mary E. Barr,**[§] **Robert P. Houser,**[||] **William B. Tolman,**[||] **Donita Sanders,**[⊥] **and James A. Fee**[⊥]

Contribution from the Department of Biochemistry and Molecular Biology, Oregon Graduate Institute of Science and Technology, P.O. Box 91000, Portland, Oregon 97291-1000, Department of Microbiology and Enzymology, Technical University of Delft, Julianalaan 67, 2628 BC Delft, The Netherlands, Chemical Sciences and Technology Division, Los Alamos National Laboratory, Mail Stop C345, Los Alamos, New Mexico 87545, Department of Chemistry and Center for Metals in Biocatalysis, University of Minnesota, 207 Pleasant Street SE, Minneapolis, Minnesota 55455, and Department of Biology, University of California at San Diego, La Jolla, California 92093

Received February 18, 1997[⊗]

Abstract: Cytochrome oxidase is the terminal oxidase in both prokaryotic and eukaryotic cells and is responsible for the generation of cellular energy via the process known as oxidative phosphorylation. The enzyme contains two Fe and three Cu centers which together provide the redox machinery for the reduction of O_2 to water. Recently, X-ray crystallography has provided the first three-dimensional description of the coordination spheres of the metal centers. However, the structures show the metal sites at low resolution, and in order to fully understand the mechanism of the reaction, it is desirable to determine the metrical details (bond lengths and angles) to much higher precision. X-ray absorption spectroscopy is unique in its ability to provide such detail, and we have applied the technique to determining the structure of the Cu$_A$ center, a thiolate-bridged binuclear copper cluster in which the coppers are bridged by two cysteine ligands and have an extremely short Cu−Cu distance of ∼2.4 Å. X-ray absorption spectroscopy, which had previously predicted the short Cu−Cu distance, has been used to further refine the structural details of the site in both the mixed-valence and fully reduced forms of the enzymes from *Thermus thermophilus* and *Bacillus subtilis*. The results have defined the structure of the Cu$_A$ core as a Cu$_2$S$_2$ diamond with Cu−S bond lengths of 2.3 Å, Cu−Cu = 2.44 Å, and very acute Cu−S−Cu angles of 65°. One-electron reduction produces only minor changes in the core geometry, with the Cu−S and Cu−Cu bond lengths increasing to 2.33 and 2.51 Å, respectively, but with the Cu−S−Cu angle remaining unchanged at 65°. The unusually high Cu−S Debye−Waller terms imply that there is significant asymmetry in the Cu$_2$S$_2$ diamond core derived from inequivalent Cu−S bond lengths. Both the metrical parameters and the temperature dependence of the Debye−Waller factors exhibit subtle differences between the mixed-valence and fully reduced proteins which suggest that the short distance may be the result, in part, of a weak metal−metal bond. The results suggest that the function of the unusual Cu$_A$ cluster is to provide a site with minimal structural perturbation occurring during electron transfer. Thus, they provide an excellent rationalization for the very low reorganizational energy, λ, observed for the Cu$_A$ center.

Introduction

The heme−copper oxidases are members of a superfamily of proton-pumping metalloenzymes found in both prokaryotic and eukaryotic organisms, which couple the energy released from the 4e$^-$ reduction of dioxygen to water to the formation of a proton motive force across the membrane which can be used for the synthesis of ATP.[1,2] The most-widely studied is the class of oxidases found in mammalian mitochondria, yeasts, and a number of bacterial systems such as *Thermus thermophilus*,[3] *Rhodobacter spheroides*,[4,5] and *Paracoccus denitri-*

ficans.[6−8] This branch of the superfamily utilizes cytochrome *c* as the electron-donating substrate and contains three redox centers: Cu$_A$ (thiolate-bridged binuclear mixed-valence center), heme *a* (6-coordinate low spin), and the dioxygen-binding heme a_3−Cu$_B$ (magnetically coupled, $S = 2$ binuclear center). A second major branch of the family, exemplified by the cytochrome bo_3 and aa_3-600 oxidases of *Escherichia coli*[1,2,9] and *Bacillus subtilis*,[10,11] respectively, uses ubiquinol as its reducing substrate, and in these cases, the Cu$_A$-binding site is absent. A

* E-mail: ninian@amethyst.cbs.ogi.edu. FAX: 503-690-1464.
† Oregon Graduate Institute.
‡ Technical University of Delft.
§ Los Alamos National Laboratory.
|| University of Minnesota.
⊥ University of California.
⊗ Abstract published in *Advance ACS Abstracts,* June 15, 1997.
(1) Hosler, J. P.; Ferguson-Miller, S.; Calhoun, M. W.; Thomas, J. W.; Hill, J.; Lemieux, L.; Ma, J.; Georgiou, C.; Fetter, J.; Shapleigh, J.; Tecklenburg, M. M. J.; Babcock, G. T.; Gennis, R. B. *J. Bioenerg. Biomembr.* **1993**, *25*, 121−136.
(2) Calhoun, M. W.; Thomas, J. W.; Gennis, R. B. *Trends Biochem. Sci.* **1994**, *19*, 325−330.

(3) Fee, J. A.; Yoshida, T.; Surerus, K. K.; Mather, M. W. *J. Bioenerg. Biomembr.* **1993**, *25*, 103−114.
(4) Shapleigh, J. P.; Hosler, J. P.; Tecklenburg, M. M. J.; Kim, Y.; Babcock, G. T.; Gennis, R. B.; Ferguson, M. S. *Proc. Natl. Acad. Sci. U.S.A.* **1992**, *89*, 4786−4790.
(5) Shapleigh, J. P.; Hill, J. J.; Alben, J. O.; Gennis, R. B. *J. Bacteriol.* **1992**, *174*, 2338−2343.
(6) Lappalainen, P.; Aasa, R.; Malmstrom, B. G.; Saraste, M. *J. Biol. Chem.* **1993**, *268*, 26416−26421.
(7) Mueller, M.; Schlaepfer, B.; Azzi, A. *Proc. Natl. Acad. Sci. U.S.A.* **1988**, *85*, 6647−6651.
(8) Steinruecke, P.; Steffens, G. C. M.; Panskus, G.; Buse, G.; Ludwig, B. *Eur. J. Biochem.* **1987**, *167*, 431−439.
(9) Minghetti, K. C.; Goswitz, V. C.; Gabriel, N. E.; Hill, J. J.; Barassi, C. A.; Georgiou, C. D.; Chan, S. I.; Gennis, R. B. *Biochemistry* **1992**, *31*, 6917−6924.

third branch, conforming to a cbb_3 distribution of hemes and containing a heme $b-Cu_B$ binuclear site, has recently been described.[12]

The bacterial oxidases contain either two or three subunits which bear homology to the mitochondrially encoded subunits I−III of the mammalian enzymes. There is remarkable sequence homology between subunit I of all members of the superfamily, and it is now established that the heme a and binuclear heme a_3-Cu_B redox centers reside within this subunit. Site-directed mutagenesis, spectroscopy, and three-dimensional modeling correctly predicted the structure and connectivity of these redox centers[1] which were recently revealed in detail by X-ray crystal structures of beef heart[13] and *P. denitrificans*[14] enzymes, both at 2.8-Å resolution. The Cu_A center of the caa_3 oxidases is located in subunit II, ∼20 Å from the subunit I redox triad.

Cu_A has attracted much interest because of its unusual spectroscopic properties[15−17] and because it is believed to be the initial site of electron entry into the oxidase.[18−20] The X-ray crystal structures have revealed that Cu_A is a unique metal center, with two thiolate groups from cysteine ligands bridging between two copper atoms. Of special interest is the very short Cu−Cu distance of ∼2.5 Å. Historically, the nuclearity of the site evoked spirited debate.[16,21−23] While early studies favored a mononuclear model, the binuclear model gradually gained acceptance. This was due largely to the work of Antholine, Kroneck, Zumft, and co-workers, who demonstrated the similarity of the EPR spectra of Cu_A in cytochrome oxidase and the A center of nitrous oxide reductase (N_2OR) which exhibits a seven-line hyperfine pattern in the $g_\parallel$ region interpreted as arising from a mixed-valence $Cu^{1.5}\cdots Cu^{1.5}$ center, with spin $S = 1/2$ delocalized over two copper nuclei.[24−27] A binuclear formulation of the Cu_A center also explained a number of studies on the metal composition which indicated that the Cu:Fe binding ratio was always greater than 2:2.[28−32] Despite these insights, spectral overlap between heme and copper signals limited the amount of structural information available on the nature of the Cu_A center in intact caa_3 preparations.

In a different approach, soluble Cu_A-binding domains were expressed by a variety of methods.[33] These include reintroduction of a Cu_A site into subunit II of the *E. coli* quinol oxidase by site-directed mutagenesis, forming the so-called cyoA construct,[34,35] and expression of soluble fragments of subunit II of *P. denitrificans*,[6] *B. subtilis*,[36] and *T. thermophilus*[37] in *E. coli*. UV/vis,[6,34,35] EPR,[36,38,39] and resonance Raman[40−43] spectroscopic studies on the copper-reconstituted forms of these recombinant Cu_A-binding proteins confirmed the strong spectral similarity between Cu_A and the A center of N_2OR, while mass spectrometric measurements indicated peaks at 126−128 mass units above those of the apoproteins, as expected for a binuclear copper site. Mutagenesis experiments implicated two cysteines, two histidines, and a methionine as the only important copper-binding ligands[35] and a number of acidic residues as binding sites for cytochrome c.[44] An EXAFS study of the soluble subunit II from *B. subtilis* from our own laboratory (reported prior to the crystal structure) proposed a unique directly bonded Cu−Cu unit (Cu−Cu = 2.5 Å) in order to explain the strong EXAFS wave which was always present at $R \approx 2.6$ Å.[45] Our EXAFS analysis indicated that, while the fit involving Cu−Cu at 2.5 Å was not unique and that Cu−S at 2.65 Å also gave an adequate simulation, the Cu−Cu interaction provided a better interpretation of all the data. We proposed a model for Cu_A involving a mixed-valence $Cu^{1.5}\cdots Cu^{1.5}$ unit in which each copper was coordinated to one His and one S(Cys). To satisfy the expected 4-coordination at copper, we suggested that the short Cu−Cu gave rise to a Cu−Cu bond, the first such bond to be observed in a biological system. Additional coordination by a Met and a Glu residue was also suggested, although these interactions were not observed by EXAFS. Parallel MCD studies on these soluble constructs by Thompson and co-workers led to the conclusion that there were only two viable structural models for Cu_A, *viz.* our directly bonded Cu−Cu proposal and

(10) Santana, M.; Kunst, F.; Hullo, M. F.; Rappoport, G.; Danchin, A.; Glaser, P. *J. Biol. Chem.* **1992**, *267*, 10225−10231.

(11) Lauraeus, M.; Haltia, T.; Saraste, M.; Wikstrom, M. *Eur. J. Biochem.* **1991**, *197*, 699−705.

(12) Wang, J.; Gray, K. A.; Daldal, F.; Rousseau, D. L. *J. Am. Chem. Soc.* **1995**, *117*, 9363−9364.

(13) Tsukihara, T.; Aoyama, H.; Yamashita, E.; Tomizaki, T.; Yamaguchi, H.; Shinzawa-Itoh, K.; Nakashima, R.; Yaono, R.; Yoshikawa, S. *Science* **1995**, *269*, 1069−1074.

(14) Iwata, S.; Ostermeier, C.; Ludwig, B.; Michel, H. *Nature* **1995**, *376*, 660−669.

(15) Malmstrom, B. G.; Aasa, R. *FEBS Lett.* **1993**, *325*, 49−52.

(16) Palmer, G. *J. Bioenerg. Biomembr.* **1993**, *25*, 145−151.

(17) Malmstrom, B. G. *Arch. Biochem. Biophys.* **1990**, *280*, 233−241.

(18) Hill, B. C. *J. Biol. Chem.* **1991**, *266*, 2219−2226.

(19) Hill, B. C. *J. Biol. Chem.* **1994**, *269*, 2419−2425.

(20) Adelroth, P.; Brezinski, P.; Malmstrom, B. G. *Biochemistry* **1995**, *34*, 2844−2849.

(21) Musser, S. M.; Stowell, M. H. B.; Chan, S. I. *Adv. Enzymol. Relat. Areas Mol. Biol.* **1995**, *71*, 79−208.

(22) Kroneck, P. M. H.; Antholine, W. E.; Koteich, H.; Kastrau, D. H. W.; Neese, F.; Zumft, W. G. In *Bioinorganic Chemistry of Copper*; Karlin, K. D., Tyeklar, Z., Eds.; Chapman & Hall: New York, 1993; pp 419−426.

(23) Li, P. M.; Malmstrom, B. G.; Chan, S. I. *FEBS Lett.* **1989**, *248*, 210−211.

(24) Kroneck, P. H. M.; Antholine, W. E.; Riester, J.; Zumft, W. G. *FEBS Lett.* **1988**, *242*, 70−74.

(25) Riester, J.; Zumft, W. G.; Kroneck, P. M. H. *Eur. J. Biochem.* **1989**, *178*, 751−762.

(26) Kroneck, P. M.; Antholine, W. E.; Kastrau, D. H. W.; Buse, G.; Steffens, G. C. M.; Zumft, W. G. *FEBS Lett.* **1990**, *268*, 274−276.

(27) Antholine, W. E.; Kastrau, D. H. W.; Steffens, G. C. M.; Buse, G.; Zumft, W. G.; Kroneck, P. M. H. *Eur. J. Biochem.* **1992**, *209*, 875−881.

(28) Einarsdottir, O.; Caughey, W. S. *Biochem. Biophys. Res. Commun.* **1985**, *129*, 840−847.

(29) Bombelka, E.; Richter, F. W.; Stroh, A.; Kadenbach, B. *Biochem. Biophys. Res. Commun.* **1986**, *140*, 1007−1014.

(30) Oblad, M.; Selin, E.; Malmstrom, B.; Strid, L.; Aasa, R.; Malmstrom, B. G. *Biochim. Biophys. Acta* **1989**, *975*, 267−270.

(31) Pan, L. P.; Zhuyin, L.; Larsen, R.; Chan, S. I. *J. Biol. Chem.* **1991**, *266*, 1367−1370.

(32) Steffens, G. C. M.; Soulimane, T.; Wolff, G.; Buse, G. *Eur. J. Biochem.* **1993**, *213*, 1149−1157.

(33) Lappalainen, P.; Saraste, M. *Biochim. Biophys. Acta* **1994**, *1187*, 222−225.

(34) van der Oost, J.; Lappalainen, P.; Musacchio, A.; Warne, A.; Lemieux, L.; Rumbley, J.; Gennis, R. B.; Aasa, R.; Pascher, T.; Malmstrom, B. G.; Saraste, M. *EMBO J.* **1992**, *11*, 3209−3217.

(35) Kelly, M.; Lappalainen, P.; Talbo, G.; Haltia, T.; van der Oost, J.; Saraste, M. *J. Biol. Chem.* **1993**, *268*, 16781−16787.

(36) von Wachenfeldt, C.; de Vries, S.; van der Oost, J. *FEBS Lett.* **1994**, *340*, 109−113.

(37) Slutter, C. E.; Sanders, D.; Wittung, P.; Malmstrom, B. G.; Aasa, R.; Richards, J. H.; Gray, H.; Fee, J. A. *Biochemistry* **1996**, *35*, 3387−3395.

(38) Neese, F.; Zumft, W. G.; Antholine, W. G.; Kroneck, P. M. H. *J. Am. Chem. Soc.* **1996**, *118*, 8692−8699.

(39) Karpefors, M.; Slutter, C. E.; Fee, J. A.; Aasa, R.; Kallebring, B.; Larsson, S.; Vanngard, T. *Biophys. J.* **1996**, *71*, 2823−2829.

(40) Andrew, C. R.; Han, J.; de Vries, S.; van der Oost, J.; Averill, B. A.; Loehr, T. M.; Sanders Loehr, J. *J. Am. Chem. Soc.* **1994**, *116*, 10805−10806.

(41) Andrew, C. R.; Lappalainen, P.; Saraste, M.; Hay, M. T.; Lu, Y.; Dennison, C.; Canters, G. W.; Fee, J. A.; Slutter, C. E.; Nakamura, N.; Sanders-Loehr, J. *J. Am. Chem. Soc.* **1995**, *117*, 10759−10760.

(42) Andrew, C. R.; Fraczkiewicz, R.; Czernuszewicz, R. S.; Lappaleinen, P.; Saraste, M.; Sanders-Loehr, J. *J. Am. Chem. Soc.* **1996**, *118*, 10436−10445.

(43) Andrew, C. R.; Sanders-Loehr, J. *Acc. Chem. Res.* **1996**, *29*, 365−372.

(44) Lappalainen, P.; Watmough, N. J.; Greenwood, C.; Saraste, M. *Biochemistry* **1995**, *34*, 5824−5830.

(45) Blackburn, N. J.; Barr, M. E.; Woodruff, W. H.; van der Oost, J.; de Vries, S. *Biochemistry* **1994**, *33*, 10401−10407.
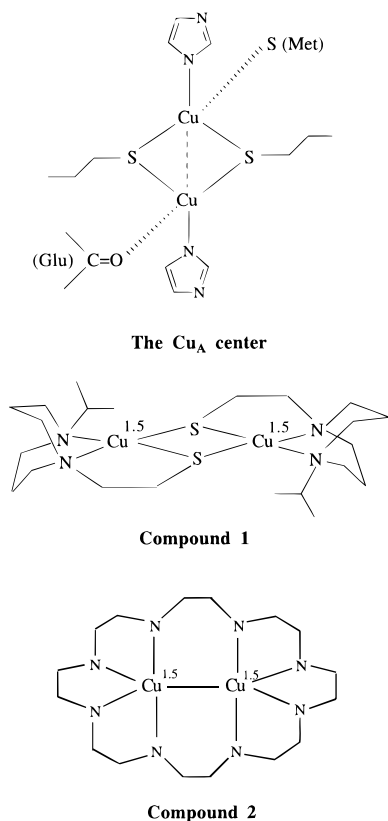
Soluble Cu_A Domains of Cytochrome c Oxidase

J. Am. Chem. Soc., Vol. 119, No. 26, 1997 6137

The Cu_A center

Compound 1

Compound 2

Figure 1. Schematic representation of the structure of the Cu_A center and the model compounds ($L^{iPrdacoS}Cu)^{2+}$ (**1**), and $(LCu_2)^{3+}$ (**2**).

an alternative involving a bis(thiolate) bridge between the two Cu atoms.[33,46]

The crystal structure of the cyoA Cu_A construct[47] has revealed the Cu_A site at higher (2.5 Å) resolution, providing dramatic confirmation of the spectroscopic predictions (Figure 1). The site is indeed dinuclear, with the two conserved cysteine residues forming a unique bis(thiolate) bridge between the two coppers, each of which is further coordinated to a single terminal histidine. The near tetrahedral coordination of each Cu is completed by a methionine and a peptide carbonyl O from a glutamic acid residue. The Cu–Cu distance is short (2.48 Å), in good agreement with the EXAFS data (see below).

The structural details of the Cu_A center, as revealed by crystallography, have posed a number of important questions. First, do the variations in Cu–Cu distance (2.7 Å, beef heart; 2.6 Å, *P. denitrificans*; 2.48 Å, cyoA) represent real structural differences, or do they merely reflect differences in crystallographic resolution? Second, what structural changes accompany reduction of the mixed-valence to the fully reduced forms of Cu_A? Third, what advantage with respect to the electron transfer (ET) mechanism does the thiolate-bridged binuclear Cu_A cluster possess relative to a mononuclear blue copper site? Fourth, does the short Cu–Cu distance truly imply the presence of a metal–metal bond as we originally suggested?[45] To answer these questions we have extended our earlier XAS studies to include structural analysis of mixed-valence and fully reduced forms of the Cu_A centers of *B. subtilis*, *T. thermophilus*, and two relevant crystallographically characterized model complexes. The results have shown that there is strong structural homology between Cu_A centers in their mixed-valence and fully reduced forms. Furthermore, the temperature

dependence of the Debye–Waller (DW) terms for the Cu–Cu and Cu–S interactions may provide additional evidence for a Cu–Cu bonding interaction in the mixed-valence state but seem to rule it out in the fully reduced state. The results have been interpreted in terms of an ET mechanism which requires minimal reorganization energy between mixed-valence and fully reduced forms.

Materials and Methods

Preparation of Protein Samples. *B. subtilis* Cu_A was prepared as described by von Wachenfeldt et al.[36] The soluble Cu_A-binding domain contained three coppers per protein, two of which comprised the binuclear Cu_A cluster and one of which was adventitiously bound copper. The adventitious copper resisted efforts to remove it by dialysis or chelation. Samples of the purple mixed-valence ($Cu^{1.5}\cdots Cu^{1.5}$) protein were concentrated to ~1.2 mM in total copper for EXAFS measurements. Samples of the colorless ($Cu^I\cdots Cu^I$) derivative were prepared by reduction with sodium ascorbate. This treatment led to complete elimination of the EPR signals characteristic of the mixed-valence derivative and of the adventitious copper.

T. thermophilus Cu_A from cytochrome ba_3 was prepared according to Slutter et al.[37] In contrast to *B. subtilis*, the soluble Cu_A-binding domain contained only the two copper atoms of the binuclear Cu_A center. The purple mixed-valence derivative was concentrated to ~5 mM in copper. Samples of the colorless reduced protein were prepared by treatment with sodium ascorbate at pH 7.8, 0.1 M Tris-HCl, 20% ethylene glycol.

X-ray Absorption (XAS) Data Collection and Analysis. XAS data were collected at the Stanford Synchrotron Radiation Laboratory (SSRL) on beam line 7.3, with a beam energy of 3 GeV and maximum stored beam currents between 100 and 50 mA. The Si(220) mono-chromator was detuned 50% to reject harmonics. The protein samples were measured as frozen aqueous glasses in 20% glycerol (*B. subtilis*) or 20% ethylene glycol (*T. thermophilus*), $T = 10-20$ K, in fluorescence mode using a 13-element Ge detector. To avoid detector saturation, the count rate of each detector channel was kept below 35 KHz for *B. subtilis* or below 100 KHz for *T. thermophilus,* for which a new high-count rate 13-element Ge detector was used. The count rate was controlled by adjusting the hutch entrance slits or by moving the detector in or out from the cryostat windows. Under these conditions, no dead-time correction was necessary. The summed data for each detector was then inspected, and only those channels that gave high-quality backgrounds free from glitches, drop outs, or scatter peaks were included in the final average. The number of scans included in the averaged spectra were as follows: *T. thermophilus* mixed-valence and fully reduced, four scans; *B. subtilis* mixed-valence and fully reduced, 21 scans.

XAS data on model compounds were measured in transmission mode. Solid samples of the model compounds were thoroughly mixed with an equal mass of boron nitride using a pestle and mortar and then pressed into rectangular aluminum sample holders (18 × 5 × 1 mm) with mylar tape windows. The averaged data were background subtracted and normalized to the smoothly varying background atomic absorption using the EXAFS data reduction package EXAFSPAK.[48] The experimental energy threshold ($k = 0$) was chosen as 8985 eV. Energy calibration was achieved by reference to the first inflection point of a copper foil (8980.3 eV) placed between the second and third ion chambers. In any series of scans, the measured energy of the first inflection of the copper foil spectrum varied by less than 1 eV. Averaged EXAFS data were referenced to the copper calibration of the first scan of a series, since the energy drift in any series of scans was too small to perturb the EXAFS oscillations. For edge analysis, four scans with absolute energy calibrations which varied by less than ±0.2 eV were averaged.

Data analysis was carried out by least-squares curve fitting utilizing full curved-wave calculations as formulated by the SRS library program EXCURV,[49–52] using methodology described in detail in previous papers from this laboratory.[53–55] The parameters refined in the fit were

(46) Farrar, J. A.; Lappalainen, P.; Zumft, W. G.; Saraste, M.; Thompson, A. J. *Eur. J. Biochem.* **1995**, *232*, 294–303.

(47) Wilmanns, M.; Lappalainen, P.; Kelly, M.; Sauer-Eriksson, E.; Saraste, M. *Proc. Natl. Acad. Sci. U.S.A.* **1995**, *92*, 11955–11959.

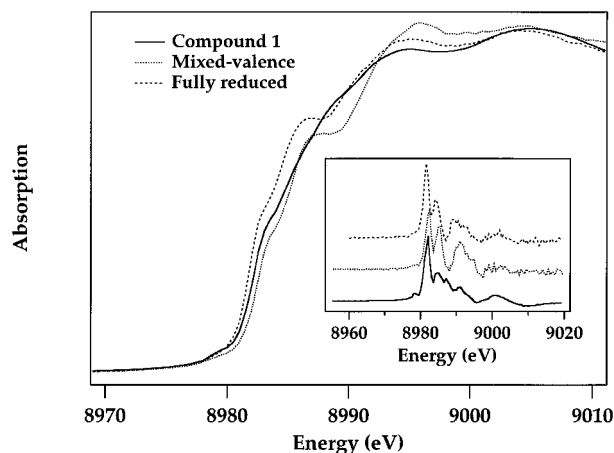(48) George, G. N. "EXAFSPAK," Stanford Synchrotron Radiation Laboratory, 1990.

Figure 2. Comparison of the Cu K-edges of mixed-valence and fully reduced *T. thermophilus* Cu$_A$ and compound **1**. The first derivatives of the absorption edges are shown in the inset.

as follows: E_0, the photoelectron energy threshold; R_i, the distance from Cu to atom *i*; and $2\sigma^2_i$, the DW term for atom *i*. Coordination numbers were fixed at the values determined from the crystal structures. The quality of the fits was determined using a least-squares fitting parameter, *F*, defined as

$$F^2 = (1/N)\sum k^6(\chi_i^{\text{theor}} - \chi_i^{\text{exp}})^2$$

referred to as the fit index.

Results and Discussion

The objectives of the work described in this paper were to compare the metrical parameters of the unique Cu$_A$ bis(thiolate)-bridged core of two different Cu$_A$-binding systems and two relevant model compounds. To this end, we have measured and interpreted the X-ray absorption spectra of both the mixed-valence (Cu$^{1.5}$···Cu$^{1.5}$) and the fully reduced (Cu^I···Cu^I) forms of *T. thermophilus* and *B. subtilis* Cu$_A$-binding soluble subunit II domains. To calibrate our analysis, we have also studied the EXAFS of two inorganic model complexes whose structures are compared with that of Cu$_A$ in Figure 1. The first of these is the bis(thiolate)-bridged fully electron-delocalized Cu$_A$ model complex, **1**, recently described by the Tolman laboratory.[56] The second is the octaazacryptand electron-delocalized complex, **2**, described by Barr and co-workers.[57] The temperature dependences of the DW factors of both the proteins and the models, particularly Cu−S and Cu−Cu DW terms, have also been investigated and have provided insights into the nature of the Cu−Cu interaction within the Cu$_2$S$_2$ core.

Absorption Edges. Figure 2 compares the Cu K-edges of compound **1**, mixed-valence and fully reduced *T. thermophilus* Cu$_A$. Inspection of the absorption data indicates strong similarities between all three spectra, most evident in the first derivative

(49) Binsted, N.; Gurman, S. J.; Campbell, J. W. *Daresbury Laboratory EXCURV88 Program*, 1988.

(50) Gurman, S. J. In *Synchrotron Radiation and Biophysics*; Hasnain, S. S., Ed.; Ellis Horwood Ltd.: Chichester, U.K., 1989; pp 9−42.

(51) Gurman, S. J.; Binsted, N.; Ross, I. *J. Phys. C* **1984**, *17*, 143−151.

(52) Gurman, S. J.; Binsted, N.; Ross, I. *J. Phys. C* **1986**, *19*, 1845−1861.

(53) Strange, R. W.; Blackburn, N. J.; Knowles, P. F.; Hasnain, S. S. *J. Am. Chem. Soc.* **1987**, *109*, 7157−7162.

(54) Blackburn, N. J.; Hasnain, S. S.; Pettingill, T. M.; Strange, R. W. *J. Biol. Chem.* **1991**, *266*, 23120−23127.

(55) Sanyal, I.; Karlin, K. D.; Strange, R. W.; Blackburn, N. J. *J. Am. Chem. Soc.* **1993**, *115*, 11259−11270.

(56) Houser, R. P.; Young, V. G. J.; Tolman, W. B. *J. Am. Chem. Soc.* **1996**, *118*, 2101−2102.

(57) Barr, M. E.; Smith, P. H.; Antholine, W. E.; Spencer, B. *J. Chem. Soc., Chem. Commun.* **1993**, 1649−1652.

data shown in the inset. Two prominent features can be identified on the rising edge of the protein spectra: 8983.2 and 8987.8 eV (inflection points from first derivatives, 8982.5 and 8985.3 eV) for mixed-valence; 8982.5 and 8986.6 eV (inflection points, 8981.6 and 8984.2 eV) for fully reduced. Thus the edges of the mixed-valence and fully reduced derivatives are essentially identical except for a ∼1 eV shift to lower energy in fully reduced. This shift is less than that usually observed for reduction of Cu(II) to Cu(I) sites in enzymes and models[58] which can be as much as 5 eV for systems involving only N and O ligands, where the charge is localized and the bonding primarily electrostatic. The observed small shift most likely reflects the complete delocalization of electronic charge over the Cu$_2$S$_2$ core. The lower energy component is also clearly visible on the absorption edge of **1** at the identical energy to mixed-valence Cu$_A$, although the higher energy peak in **1** is very weak and its energy poorly defined. The similarity of the edge data suggests strong similarities in geometric and electronic structure. A weak 1s → 3d quadrupolar transition is evident in the spectra of **1** and mixed-valence Cu$_A$ at 8979.5 eV, with the intensity of the protein about one-half that of the model.

EXAFS Studies on Cu$_A$ Model Compounds. Compound **1** is the closest available model for Cu$_A$. The complex accurately mimics the electron-delocalized mixed-valence redox state and provides the bis(thiolate) bridging geometry characteristic of the Cu$_A$ core. However, the Cu−Cu distance in the model (2.93 Å) is not as short as in the protein (∼2.5 Å), with significantly less acute Cu−S−Cu bridging angles. Compound **2**, on the other hand, exhibits a very short Cu−Cu interaction (2.41 Å). The lack of any coordinated bridging ligands implicates Cu−Cu bonding as the origin of the strong Cu−Cu interaction. Both complexes thus model different elements of the Cu$_A$ site. In previous work from this laboratory, in which EXAFS evidence for a short Cu−Cu interaction was first presented,[45] the simulation methodologies had underestimated by 0.07 Å the Cu−Cu interaction in the octaazacryptand dicopper[1.5] complex, **2**, used to model the very short Cu−Cu distance in the protein. It was believed that this discrepancy was due to a small inaccuracy in the copper phase shift.

To provide a firm basis for interpreting and comparing the Cu−Cu distances among different Cu$_A$ constructs, we first carefully investigated the EXAFS of **1**. Initial attempts to simulate the data using the program EXCURV gave good correspondence between crystallographic and EXAFS-derived Cu−N and Cu−S distances, but again indicated a 0.07 Å underestimation of the Cu−Cu distance. The Cu−Cu distance was therefore recalibrated by refinement of the copper scatterer phase shift such that the correct distance was obtained by the simulation procedure. Figure 3a shows the Fourier transform and EXAFS (inset) of the best fit obtained by this protocol. Agreement with experiment and theory is excellent over the complete range of the data ($k = 3−16$ Å^{-1}). The refined copper scatterer phase shift was then tested by simulation of the EXAFS of complex **2**. The results are shown in Figure 3b, where the simulation produced a Cu−Cu distance of 2.41 Å, in close agreement with the crystallographic distance of 2.415 Å. Table 1 compares the EXAFS-derived distances with their crystallographic counterparts, showing satisfactory agreement. This analysis confirms that the refined copper phase shift gives accurate Cu−Cu distances and can be used with confidence in the analysis of the protein data.

EXAFS of *T. thermophilus* Cu$_A$. The EXAFS and Fourier transforms of mixed-valence and fully reduced *T. thermophilus*

(58) Boswell, J. S.; Reedy, B. J.; Kulathila, R.; Merkler, D. J.; Blackburn, N. J. *Biochemistry* **1995**, *35*, 12241−12250.
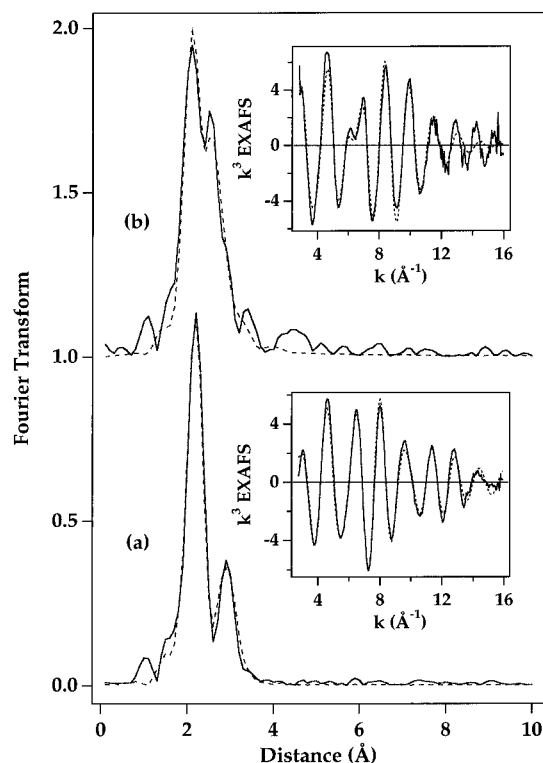
Figure 3. EXAFS of model compounds **1** and **2**: (a) simulated versus experimental Fourier transforms and EXAFS (inset) of compound **1** and (b) simulated versus experimental Fourier transforms and EXAFS (inset) of compound **2**.

Table 1. EXAFS Analysis of Model Complexes **1** and **2**[a]

		1			**2**	
	N	R_{EXAFS}	R_{CRYST}	N	R_{EXAFS}	R_{CRYST}
Cu−N	2	2.15	2.12	4	2.07	2.07
Cu−S	2	2.25	2.27			
Cu−Cu	1	2.93	2.93	1	2.41	2.41
Cu−C				6	2.75	2.85
Cu−C				9	3.19	3.24

[a] Comparison of EXAFS-derived distances (Å) with crystallography. Compound **1** was used to refine the Cu phase shift in simulations using the program EXCURV as described in the text.

Cu$_A$ are shown in Figure 4. The data exhibit strong oscillations out to $k = 15$ due to the strong contributions from both Cu−S and Cu−Cu components. The crystal structures have defined the coordination as shown in Figure 1. For the purposes of simulating the EXAFS data, we have therefore fixed the coordination numbers at each copper at 1 N from the terminal histidine, 2 S from the bridging cysteines, and 1 Cu. Refinement of distances and DW terms for these three shells gives the fits shown in Figure 4 and Table 2. No evidence was found for EXAFS contributions from either a coordinated methionine or an oxygen from a main chain carbonyl of a glutamate residue. For the mixed-valence protein, the Cu−N and Cu−S distances are 1.96 and 2.29 Å, respectively. The Cu−S distance is typical of copper thiolate coordination[56,59,60] and close to that found in the model complex **1**. The Cu−N distance is about 0.2 Å shorter than the Cu−N distance in **1**, and this may reflect the fact that the Cu$_A$ site is pseudo 3-coordinate. The Cu−Cu distance at 2.43 Å is the shortest metal−metal distance found in any metalloprotein system and approaches that found in the macrocyclic metal−metal bonded complex **2**. As previously
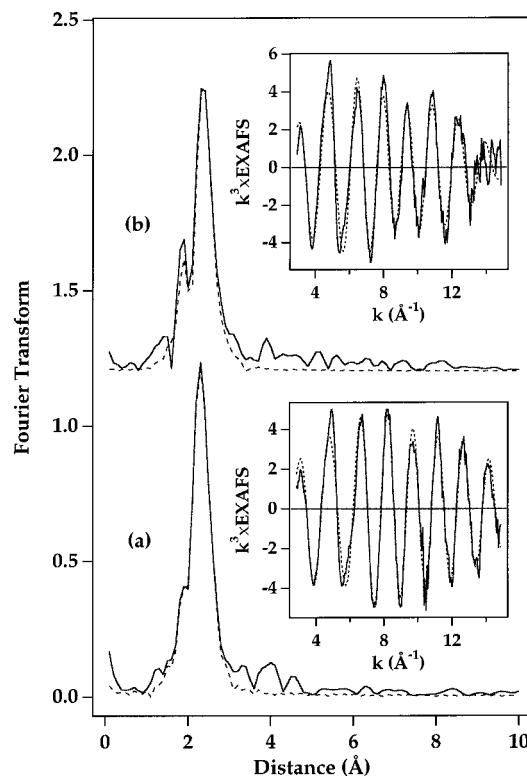
(59) Houser, R. P.; Tolman, W. B. *Inorg. Chem.* **1995**, *34*, 1632−1633.
(60) Houser, R. P.; Halfen, J. A.; Young, V. G. J.; Blackburn, N. J.; Tolman, W. B. *J. Am. Chem. Soc.* **1995**, *117*, 10745−10746.

Figure 4. EXAFS of *T. thermophilus* Cu$_A$: (a) simulated versus experimental Fourier transforms and EXAFS (inset) of mixed-valence protein and (b) simulated versus experimental Fourier transforms and EXAFS (inset) of fully reduced protein.

suggested,[45] this raises the question of whether a true metal−metal bond exists in the Cu$_A$ binuclear site. The metrical parameters determined for the fully reduced form of the *T. thermophilus* Cu$_A$ center indicate subtle changes at the dicopper cluster. The fully reduced data can be simulated with an identical donor atom set, as for the mixed-valence data. The bridging Cu−S and Cu−Cu distances increase to 2.33 and 2.51 Å, respectively, while the terminal Cu−N distance remains essentially unchanged. Thus, one-electron reduction of mixed-valence Cu$_A$ produces only very minor perturbation of the cluster.

EXAFS of *B. subtilis* Cu$_A$. EXAFS data for mixed-valence and fully reduced forms of *B. subtilis* Cu$_A$ are presented in Figure 5 and Table 2. The *B. subtilis* Cu$_A$ preparation was complicated by the presence of an additional adventitious copper center, giving a total of three coppers per protein. The coordination numbers found in the EXAFS analysis therefore relate to three Cu absorbers, and the data contain the contribution from the adventitious copper. However, since the latter is most likely coordinated by O/N donors, only the Cu−N distances are expected to be affected. The EXAFS of the mixed-valence protein shows, as expected, a more intense Cu−N shell and can be well simulated by 2 N at 1.95 Å, 1.3 S at 2.30 Å, and 0.7 Cu at 2.44 Å. This distribution of shells is consistent with the Cu−S and Cu−Cu contributions arising entirely from the Cu$_A$ center, with distances identical to those of *T. thermophilus* within experimental error. For fully reduced *B. subtilis* Cu$_A$, the Cu−N coordination number drops to 1.2, suggesting a lower coordination number for the fully reduced adventitious center. The Cu−S and Cu−Cu coordination numbers remain unchanged, again consistent with these being derived entirely from the Cu$_A$ cluster. The Cu−Cu distance of 2.52 Å is the same as that found in *T. thermophilus*; the Cu−S distance, however, is

Table 2. Comparison of EXAFS-Derived Cu−N(His), Cu−S(Cys), and Cu−Cu Distances for Mixed-Valence and Fully Reduced Forms of Different Cu$_A$ Constructs at 10 K[a]

		Cu−N(His)		Cu−S(Cys)		Cu−Cu	
	fit index	R (Å^{-1})	$2\sigma^2$ (Å^2)	R (Å^{-1})	$2\sigma^2$ (Å^2)	R (Å^{-1})	$2\sigma^2$ (Å^2)
T. thermophilus[b] (mixed-valence)	0.84	1.96	0.004	2.29	0.011	2.43	0.002
T. thermophilus[b] (fully reduced)	1.47	1.97	0.001	2.33	0.014	2.51	0.007
B. subtilis[c] (mixed-valence)	1.28	1.95	0.005	2.30	0.014	2.44	0.005
B. subtilis[c] (fully reduced)	0.95	1.95	0.011	2.23	0.022	2.52	0.010
thiolate-bridged complex **1**[d]	0.34	2.15	0.011	2.25	0.009	2.93	0.013

[a] Distances are accurate to ±0.02 Å; coordination numbers are accurate to ±25%. [b] For *T. thermophilus* Cu$_A$, the coordination numbers in the simulations were fixed at 1.0 N, 2.0 S, and 1.0 Cu scatterers per Cu$_A$ absorber. [c] For *B. subtilis*, additional N/O scatterers were included to account for the adventitious copper (2.0 N/O, 1.3 S, and 0.7 Cu scatterers per Cu absorber; see text). [d] The metrical parameters used to fit the bis(thiolate)-bridged complex **1** (2.0 N, 2.0 S, and 1.0 Cu per Cu absorber) are also given for comparison.
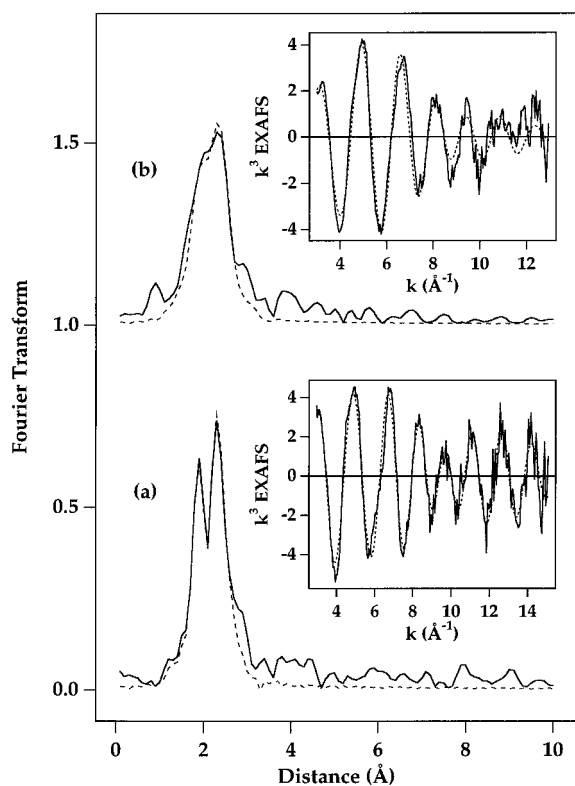

Figure 5. EXAFS of *B. subtilis* Cu$_A$: (a) simulated versus experimental Fourier transforms and EXAFS (inset) of mixed-valence protein and (b) simulated versus experimental Fourier transforms and EXAFS (inset) of fully reduced protein.

now shorter at 2.23 Å. It is not clear whether this shorter distance stems from the presence of the adventitious Cu component.

Debye−Waller Factors. The DW terms determined from the analysis of Cu$_A$ from both sources are unusual. First, the Cu−S DW terms are very large for first-shell scatterers. We have already commented on this in our previous study of *B. subtilis*, where the unusually high DW terms obtained when two S(cys) ligands were included in the fit seemed to suggest ligation of only one Cys per Cu$_A$, thus leading us to propose terminal rather than bridging ligation of the cysteine ligands. The thiolate-bridged structure clearly requires an alternative explanation for the high Cu−S DW terms. Two possible explanations are (i) a large static disorder in the Cu−S bond lengths, arising from a spread in R_{Cu-S} about the average Cu−S determined from EXAFS, or (ii) a dynamic disorder arising from thermal population of normal modes with large Cu−S vibrational components. Since the data were recorded at 10 K, the latter possibility seems less likely. The second unusual feature is the very small DW term found for the Cu−Cu interaction in the mixed-valence derivatives, which increases substantially on
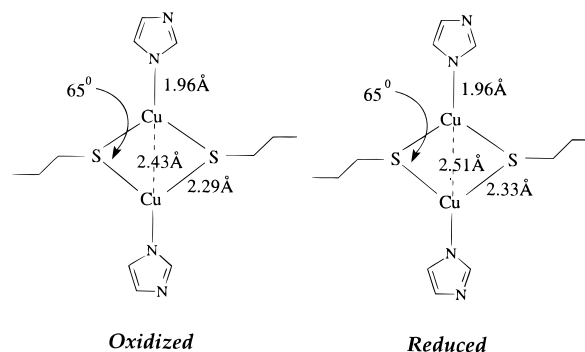

Figure 6. Comparison of the core dimensions of mixed-valence and fully reduced Cu$_A$.

reduction. This could imply that the mixed-valence forms contain an additional interaction between copper centers over that found in the fully reduced proteins and may suggest the presence of metal−metal bonding in the mixed-valence derivatives. We shall return to these points later when we discuss the temperature dependence of the DW terms.

Comparison of the Cu$_2$S$_2$ Core Structure of Mixed-Valence and Fully Reduced Cu$_A$. The data lead to a detailed metrical description of the Cu$_A$ cluster in the mixed-valence and fully reduced forms, as shown in Figure 6. The EXAFS-derived Cu−S and Cu−Cu distances allow us to calculate the Cu−S−Cu angles in the two forms. For mixed-valence Cu$_A$, the Cu$_2$S$_2$ diamond has Cu−S and Cu−Cu distances of 2.29 and 2.43 Å, respectively, leading to a Cu−S−Cu angle of 65°. In the fully reduced form, the diamond core expands slightly, as evidenced by the small increase of Cu−S and Cu−Cu to 2.33 and 2.51 Å, respectively, but the Cu−S−Cu angle remains unchanged at 65°. This suggests that the structure of the Cu$_2$S$_2$ core is highly conserved between mixed-valence and fully reduced forms and that structural reorganization accompanying cluster redox involves little more than a vibrational breathing mode of the core.

The above finding is highly significant with respect to the ET mechanism in cytochrome c oxidase. Electron transfer from cytochrome c to dioxygen bound at the Fe$_{a3}$−Cu$_B$ dinuclear center is known to proceed from cyt c → Cu$_A$ → Fe$_a$ → Fe$_{a3}$. Thus, the Cu$_A$ center is the site of initial electron entry from cytochrome c. Studies on the interaction of the *P. denitrificans* soluble subunit II domain with its biological ET partner cyt c_{550}[44] have determined a second-order rate constant of 1.5×10^6 M^{-1} s^{-1}, which is similar to the values previously observed for the reaction of the intact oxidase with its substrate cyt c. In addition, site-directed mutagenesis has implicated a number of anionic residues in cyt c_{550} binding to the Cu$_A$ domain, suggesting a single cytochrome c-binding site. These studies confirm that the ET from cyt c to Cu$_A$ occurs in a monophasic reaction involving rate-limiting binding of substrate at a single site

followed by very rapid ET.[44] A more quantitative discussion of the ET from Cu$_A$ to Fe$_a$ is available as discussed by Ramirez and co-workers.[61] These workers have identified a 16-bond (14 covalent bonds, 2 H bonds) through-bond pathway between Cu$_A$ and heme *a*, initiating on the H224 Cu$_A$ terminal ligand (*P. denitrificans* structure). Using the rate constant of 1.8×10^4 s^{-1} and reasonable values for covalent and H bond coupling efficiencies, they calculate an ET reorganizational energy, λ, between 0.15 and 0.5 eV for the Cu$_A$ center. Typical values for other protein ET reactions are in the range 0.7−1.3 eV.

These arguments suggest that the very rapid ET rates, both for the intermolecular cytochrome *c* to Cu$_A$ and for the intramolecular Cu$_A$ to heme *a* ET reactions, can be traced to an unusually low reorganizational energy, λ, for the Cu$_A$ cluster. The reorganizational energy is made up of contributions from both redox-induced structural reorganization of the cluster and from changes in the degree of solvent/polypeptide ordering around the ET site. The relatively small reaction entropy (−5.4 eu) determined from electrochemical measurements of *T. thermophilus* Cu$_A$ indicates minimal solvent ordering in the vicinity of the Cu$_A$ cluster.[62] Our EXAFS data show that structural reorganization of the cluster is small and provide a structural framework to interpret the origin of the low value of λ. The structural interconversion of mixed-valence and fully reduced Cu$_A$ centers requires only a symmetric breathing mode of the diamond core involving small displacements along the Cu−Cu and Cu−S axes, but no change in the Cu−S−Cu angle. These displacements closely parallel the atomic displacements of the lowest energy A$_{1g}$ modes calculated from a normal coordinate analysis of the Cu$_A$ resonance Raman spectrum[42] (observed experimentally at 138 and 339 cm^{-1})[42,43,63] and thus rationalize the extremely low reorganizational energy for the site.

Asymmetry of the Cu$_2$S$_2$ Core. Despite the common Cu$_2$S$_2$ core, differences exist in the optical and EPR spectra of different Cu$_A$ centers, which have been interpreted as arising from differences in site symmetry or coordination environment of the two Cu atoms.[64] While large differences in site symmetry might be expected to favor valence localization, more subtle variations in site symmetry could produce varying degrees of valence delocalization spanning the Cu$_A$ centers from different sources. The effect is most noticeable in the EPR spectra. The *E. coli* cyoA construct exhibits the highest degree of inequivalence between the two copper centers, with A_z Cu hyperfine coupling constants which differ by 1.5 mT.[64] The Cu$_A$ center of N$_2$OR is the most symmetrical, but even here the best simulations require small differences in Cu hyperfine couplings or non-colinearity of the *g* and *A* tensors of the two coppers.[38] The CD and EPR spectra of *T. thermophilus* Cu$_A$ place it toward the more symmetrical end of these extremes.[37,39,65] Farrar and co-workers have further suggested that the inequivalence in copper site symmetry is caused by differences in the Cu−O bond length of the coordinated glutamate main chain carbonyl ligand, citing as evidence the different Cu−O bond lengths of

2.3 and 3.0 Å found in the crystal structures of the *E. coli* re-engineered cyoA Cu$_A$ construct and *P. denitrificans*, respectively.

The EXAFS analysis presented here could not detect any other ligands in close proximity to either Cu. This is consistent with a weak interaction between the coordinated methionine at a distance in excess of ~2.6 Å. However, it is inconsistent with the presence of the O atom from the glutamate main-chain carbonyl at 2.3 Å from the Cu. Our analysis finds no support for the presence of an O donor at this distance. Furthermore, the Cu−N(His) distances of 1.77 and 1.85 Å reported in the cyoA Cu$_A$ crystal structure are unreasonably short for a copper center with a coordination number of 3 or greater and are clearly much shorter than the EXAFS-derived distances presented here. Although we have not measured the EXAFS of CyoA, we believe it unlikely that a weak ligand such as a main-chain carbonyl would be found at 2.3 Å, particularly as the high-resolution structures of azurins show this potential donor atom to be more than 3 Å from the copper.[66] On the other hand, the unusually high values of the Cu−S DW factors found in Cu$_A$ provide strong evidence for heterogeneity in the Cu−S bond lengths (see below). Thus, we believe that distortion of the Cu$_2$S$_2$ diamond core via inequivalence of Cu−S bond lengths provides an alternative and more plausible explanation for copper site inequivalence. Such effects have been found in oxo-bridged mixed-valence Fe^{II}/Fe^{III} dimers, where a difference of 0.04 Å in Fe−O bond lengths was sufficient to induce valence trapping.[67] Inequivalent Fe−O bond lengths have also been found in bis(μ-oxo)diiron(III) diamond cores.[68−70] We also note that Cu−S inequivalence might occur across a population of Cu$_A$ molecules, as has recently been proposed to account for the observed *g* strain in the *T. thermophilus* Cu$_A$ EPR spectrum.[39] The true situation is most likely some combination of intra- and intermolecular inequivalence of the Cu−S bond lengths of the diamond core.

Temperature Dependence of Debye−Waller Factors. The DW terms ($2\sigma^2$) for the Cu−S and Cu−Cu contributions to the EXAFS of Cu$_A$ are unusual (Table 2). The Cu−S DW terms (0.011−0.014 Å^2 for mixed-valence and fully reduced, respectively) are larger than expected for first-shell scatterers, while the Cu−Cu DW terms for the mixed-valence derivatives (0.002 Å^2, *T. thermophilus*; 0.005 Å^2, *B. subtilis*) are extremely small for metal−metal interactions. The model compounds **1** and **2** provide some indication of the range of DW terms expected in complexes of similar structure. The bis(thiolate)-bridged mixed-valence model **1** with its long (2.93 Å) Cu−Cu distance and no Cu−Cu bond shows Cu−S and Cu−Cu DW terms of 0.009 and 0.013 Å^2, respectively. Although smaller than those found for the proteins, the Cu−S DW term is still high for a first-shell scatterer in a model compound. Reference to the crystal structure shows that, of the four Cu−S bonds of the Cu$_2$S$_2$ core, two are related by the 2-fold crystallographic symmetry, but the remaining two are inequivalent with Cu−S distances of 2.25 and 2.29 Å, respectively. The EXAFS analysis (Tables 1 and 2), which treats the Cu−S component as a single unsplit shell, produces a Cu−S of 2.25 ± 0.02 Å and a DW term of 0.009 Å^2. Allowing the shell to split results in Cu−S distances of 2.21 and 2.29 Å, with a decrease in the DW to a very reasonable value of 0.004 Å^2 and no change in the fit index. Although

(61) Ramirez, B. E.; Malmstrom, B. G.; Winkler, J. R.; Gray, H. B. *Proc. Natl. Acad. Sci. U.S.A.* **1995**, *92*, 11949−11951.

(62) Immoos, C.; Hill, M. G.; Sanders, D.; Fee, J. A.; Slutter, C. E.; Richards, J. H.; Gray, H. B. *J. Biol. Inorg. Chem.* **1996**, *1*, 529−531.

(63) Wallace-Williams, S. E.; James, C. A.; de Vries, S.; Saraste, M.; Lappalainen, P.; van der Oost, J.; Fabian, M.; Palmer, G.; Woodruff, W. H. *J. Am. Chem. Soc.* **1996**, *118*, 3986−3987.

(64) Farrar, J. A.; Neese, F.; Lappalainen, P.; Kroneck, P. M. H.; Saraste, M.; Zumft, W. G.; Thompson, A. J. *J. Am. Chem. Soc.* **1996**, *118*, 11501−11514.

(65) Fee, J. A.; Sanders, D.; Slutter, C. E.; Doan, P. E.; Aasa, R.; Karpefors, M.; Vanngard, T. *Biochem. Biophys. Res. Commun.* **1995**, *212*, 77−83.

(66) Adman, E. T. *Adv. Protein Chem.* **1991**, *42*, 145−197.

(67) Cohen, J. D.; Payne, S.; Hagen, K. S.; Sanders-Loehr, J. *J. Am. Chem. Soc.* **1997**, *119*, 2960−2961.

(68) Que, L. J.; Dong, Y. *Acc. Chem. Res.* **1996**, *29*, 190−196.

(69) Zang, Y.; Dong, Y.; Que, L. J. *J. Am. Chem. Soc.* **1995**, *117*, 1169−1170.

(70) Dong, Y.; Menage, S.; Brennan, B. A.; Elgren, T. E.; Jang, H. G.; Pierce, L. L.; Que, L. J. *J. Am. Chem. Soc.* **1993**, *115*, 1851−1859.

Table 3.   Temperature Dependence of the Debye−Waller Terms ($2\sigma^2$, Å^2) for *T. thermophilus* Cu$_A$ and the Model Compounds **1** and **2**

	10 K			100 K			200 K		
	Cu−N	Cu−S	Cu−Cu	Cu−N	Cu−S	Cu−Cu	Cu−N	Cu−S	Cu−Cu
T. thermophilus (mixed valence)[a]	0.004	0.011	0.002	0.006	0.010	0.008			
T. thermophilus (fully reduced)	0.001	0.014	0.007	0.006	0.014	0.009	0.011	0.019	0.014
complex **1**	0.011	0.009	0.013	0.012	0.010	0.016	0.015	0.012	0.021
complex **2**	0.011		0.006				0.014		0.008

[a] Due to photoreduction, data for mixed-valence *T. thermophilus* Cu$_A$ could not be obtained above 100 K.

the two-shell refinement overestimates the magnitude of the Cu−S splitting on the low *R* side, it suggests that the higher than expected DW term for the Cu−S shell in **1** is due primarily to the inequivalence of the Cu−S distances.

Confirmation of this conclusion is available from the temperature dependence of the DW terms. XAS spectra were recorded for compounds **1** and **2** and for the mixed-valence and fully reduced forms of *T. thermophilus* Cu$_A$ at temperatures between 10 and 200 K. For mixed-valence Cu$_A$, photoreduction led to bleaching of the sample at temperatures above 100 K. The data were analyzed by least-squares refinement in which E_0, coordination numbers, and distances were held at the values obtained for data measured at 10 K, and all DW terms were floated in the fit. For the higher *T* data, the quality of fits obtained was equivalent to the 10 K fits as judged by nearly identical fit indices. This analysis provides quantitative data on the temperature dependence of the DW terms for each shell, and the results are summarized in Table 3.

Inequivalence of the Cu−S Distances. The *T* dependence of the Cu−S shells is very small, strongly suggesting that the high DW terms for Cu−S are due to static disorder originating from a spread in the Cu−S distances and confirming the conclusions derived from the two-shell analysis of the EXAFS of **1**. The Cu−S DW term for mixed-valence Cu$_A$ does not vary significantly between 10 and 100 K. This poses the question, do the high DW terms for Cu−S in Cu$_A$ also reflect inequivalence in the Cu−S distances of the Cu$_2$S$_2$ core? A two-shell analysis of the Cu$_A$ protein data leads to Cu−S distances (DW terms) of 2.25 Å (0.007 Å^2) and 2.33 Å (0.007 Å^2) for mixed-valence and 2.27 Å (0.006 Å^2) and 2.38 Å (0.005 Å^2) for fully reduced. Using **1** as calibration, we expect the splitting to be overestimated on the low *R* side by ∼0.04 Å, leading to an estimate for the inequivalence in Cu−S distances of 2.29−2.33 Å for mixed-valence and 2.31−2.38 Å for fully reduced. However, the 2-fold crystallographic symmetry present in the model is absent in the protein Cu$_A$ center, such that inequivalence in all four Cu−S distances is possible. This inequivalence will contribute to the reduction in site symmetry of the Cu$_A$ center observed by MCD and EPR and already discussed above.

Temperature Dependence of Cu−Cu and the Presence of Cu−Cu Bonding. The *T* dependence of the Cu−Cu DW terms can be seen in Table 3 and Figure 7. Although the data range is limited for mixed-valence *T. thermophilus* Cu$_A$ due to photoreduction above 100 K, it is clear that the Cu−Cu DW term is much smaller and has a steeper *T* dependence than fully reduced Cu$_A$ or compound **1**. This suggests that the normal mode(s) that gives rise to vibrational damping of the EXAFS oscillations induces significant change in Cu−Cu distance and, hence, must include a component of Cu−Cu stretching. On the other hand, as discussed above, the lack of measurable *T* dependence for the Cu−S components of the EXAFS of mixed-valence Cu$_A$ in this same *T* range implies little or no change in Cu−S bond length in the normal mode. These considerations suggest that the normal mode that mediates the *T* dependence is the lowest energy A$_g$ mode, identified near 140 cm^{-1} and assigned by normal coordinate analysis as either predominantly
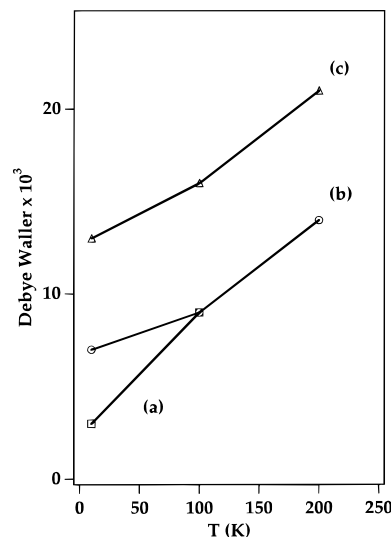

Figure 7. Temperature dependence of the Cu−Cu Debye−Waller terms: (a) mixed-valence *T. thermophilus*, (b) fully reduced *T. thermophilus*, and (c) compound **1**.
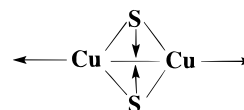

Figure 8. Lowest energy normal mode of the Cu$_2$S$_2$ diamond (from ref 43).

Cu−Cu stretching or Cu−S−Cu bending[42,43,63] (Figure 8). However, it is significant that the fully reduced Cu$_A$ has a markedly larger Cu−Cu DW term at 10 K than mixed-valence and a flatter *T* dependence which approximates that of compound **1**. The latter clearly has no Cu−Cu bond as the Cu−Cu distance is 2.93 Å. This would suggest that a more intense Cu−Cu interaction is present in the mixed-valence protein over that present in either fully reduced or compound **1**. Given the nearly identical Cu$_2$S$_2$ core structures of mixed-valence and fully reduced Cu$_A$ centers, a component of Cu−Cu bonding involving the unpaired (b$_{3u}$) d-electron[38,64] in the mixed-valence form seems a more likely explanation than an increase in Cu−S−Cu bending frequency. Thus we conclude that a possible explanation for the very small DW term in mixed-valence Cu$_A$ is the presence of a metal−metal bond.

Recent electronic structural calculations on *B. subtilis* Cu$_A$ and compound **1** have reached similar conclusions.[71] Assignment of the lowest energy electronic absorption bands as class III mixed-valence transitions has allowed the calculation of the ground-state electronic coupling energy 2H_{AB} (responsible for the valence delocalization) as 13 000 and 4800 cm^{-1} for Cu$_A$ and compound **1**, respectively. Since S K-edge spectroscopy indicated almost identical degrees of S covalency in their respective HOMOs, the additional interaction energy was

(71) Williams, K. R.; Gamelin, D. R.; Lacroix, L. B.; Houser, R. P.; Tolman, W. B.; Mulder, M. C.; de Vries, S.; Hedman, B.; Hodgson, K. O.; Solomon, E. I. *J. Am. Chem. Soc.* **1997**, *119*, 613−614.

attributed to direct overlap of Cu 3d orbitals resulting in Cu—Cu σ^b–σ^* splitting.

It follows that any Cu—Cu bond mediated primarily through interaction of 3d orbitals must be absent in the fully reduced derivative where the 3d shell is full. Despite this, the fully reduced Cu$_A$ manages to maintain the same Cu$_2$S$_2$ core structure necessary for minimizing the reorganizational energy. It is possible that some alternative description of Cu—Cu bonding is operative in the fully reduced Cu$_A$ site, such as mixing of filled d orbitals with empty 4s and 4p orbitals on Cu(I), as suggested by Merz and Hoffmann to explain the short (2.35 Å) Cu—Cu distance found in certain oligomeric Cu(I) complexes.[72] However, studies on Cu$_A$ constructs produced by loop-directed mutagenesis of azurin and amicyanin blue copper sites (to be published in full elsewhere) have indicated a much weaker Cu—Cu interaction (as measured from the magnitude of Cu—Cu DW terms) in the fully reduced forms. Thus, it would appear that

(72) Merz, K. M.; Hoffmann, R. *Inorg. Chem.* **1988**, *27*, 2120–2127.

the protein primary sequence in the vicinity of the dinuclear center is critical in influencing the relative stability of mixed-valence and fully reduced forms and in dictating the ET properties. Further studies are underway to fully explore these factors.

JA970513E